DOI:10.48011/asba.v2i1.1752

A New Discrete-Time Robust Adaptive Predictive Control-Based RMRAC Applied to Grid Connected Converters With LCL-Filter ⋆

Wagner B. da Silveira * **Deise M. C. Milbradt** *
Guilherme V. Hollweg * **Paulo J. D. O. Evald** *
Rodrigo V. Tambara * **Hilton A. Gründling** *

* *Power Electronics and Control Research Group, Federal University of Santa Maria, Santa Maria, Brasil (e-mail: wasilveira91@hotmail.com, deise.milbradt@ufsm.br, guilhermehollweg@gmail.com, paulo.evald@gmail.com, rodvarella10@gmail.com, ghilton03@gmail.com).*

Abstract:
In this work, is developed a new discrete-time robust adaptive predictive control based on combining the adaptive structure of a Model Reference Adaptive Controller (RMRAC), to adjust gains online, with the control law One Sample Ahead Preview (OSAP), a particular case of deadbeat controller, for the current loop of a grid-connected voltage-source converter, also, this control not need resonant controllers to reject exogenous disturbances. A case application is presented, the grid-side currents control of a three-phase full-bridge static converter connected to the electrical grid by LCL filter. Simulation results are presented to show the performance of the proposed controller in a grid connected system.

Keywords: Adaptive Control, Robust Control, Model Predictive Control, OSAP Control, Grid-Connected Converters, LCL Filter.

1. INTRODUCTION

The fast development of the human society and the industrial production implies on intense demand for energy and fast fossil fuels depletion Chen et al. (2019); Fang et al. (2019). Furthermore, concerns about well-being of the environment and global warming have attracted interest in deployments of renewable energy sources Malinowski et al. (2015); Jha (2016); Chowdhury (2016). Thus, Since last decade, renewable energy sector have been turning more and more relevant Kuznietsov et al. (2019).

Grid-connected power generation systems based on photovoltaic panels, wind turbines, fuel cells, among others, have used static converters with LCL filters to attenuate high harmonic frequencies Dannehl et al. (2007). For high power converters, larger than $1MW$, LCL filters are commonly employed due to their high attenuation of current harmonics, inherent to converter's switching frequency. In addition, without significantly increasing the reactive power consumed at the grid frequency compared to an L filter. Furthermore, the grid impedance causes uncertainties on LCL's resonance frequency. It is a relevant dynamics that have to be considered on controller design to ensure stability and performance of the grid-connected converter Liserre et al. (2006).

⋆ This study was financed in part by the Coordenação de Aperfeiçoamento de Pessoal de Nível Superior - Brasil (CAPES/PROEX).

As for LCL resonance damping, there are two main solutions presented on literature, to suppress it. They are: (I) the use of passive damping to attenuate the resonance peak, which is undesirable at high power systems, due to energy cost and power losses caused by insertion of passive elements on the filter. Moreover, these methods depend on the PCC (Point of Common Coupling) characteristics; (II) the use of active damping, which can be achieved through different control strategies, such as optimal controller Mariethoz et al. (2008), PI controller Lindgren and Svensson (1998) and Ponnaluri and Serpa (2008), the PI controller with resonant Liserre et al. (2006), robust control Gabe et al. (2009) and Maccari (2014) and adaptive control Massing et al. (2012); Tambara et al. (2013).

Regardless of the approach used or the control technique, it's desirable the control algorithm has the following property: capable to keep system stability and good performance even in the presence of structured and unstructured uncertainties, as well as disturbances, since the performance and stability of the closed loop system is substantially dependent on the grid parameters and the dynamics of the converter output filter.

Ioannou and Tsakalis (1986a) shows a few strategies of RMRAC controller which has been used for a lot of papers along the years to solve similar problems of grid connected converters with LCL-filter. In Tambara (2014) proposed a RMRAC discrete-time feedback state and input-output approach controller based on a modified RLS (Recursive

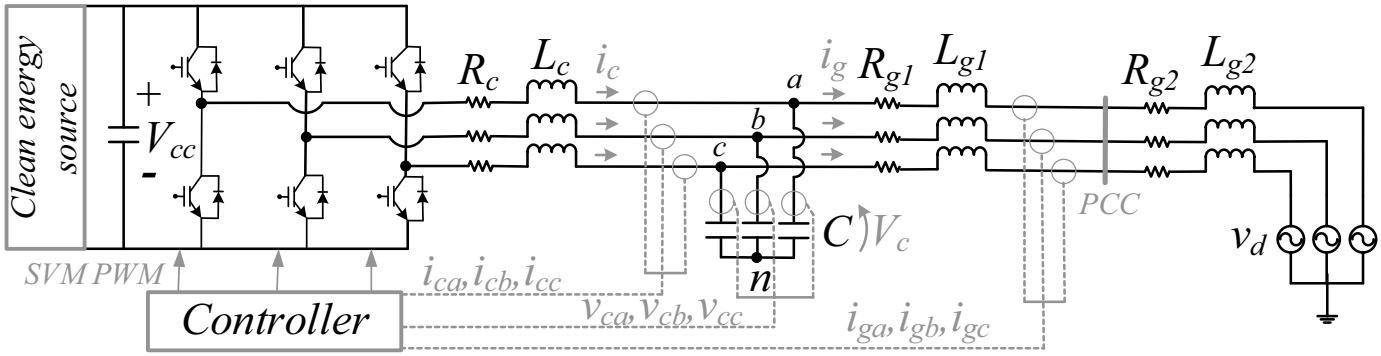

Figure 1. Grid-tied converter with LCL filter

Least Square) adaptation algorithm, to damping of the resonant peak of the LCL filter.

Recently, among these new control schemes, predictive control such as model predictive control (MPC) Exposto et al. (2015) appears to be a very interesting alternative to obtain high performance for grid-connected inverter application. In Mohamed and El-Saadany (2007), an improved deadbeat current control scheme with a novel adaptive self-tuning load model for a three phase pulse width-modulated (PWM) voltage-source inverter is proposed. Baek et al. (2015); Shi et al. (2019) present a predictive current control method and its application to a voltage source inverter. In fact, these algorithms show good results if the system is well known. By the way, if the system presents structured and unstructured uncertainties (such as unmodeled dynamics) modifications must be included in these control schemes.

In order to meet the control requirements of the high-power static converter with LCL fillter, this paper proposes a discrete time controller based on combining the adaptive structure of an RMRAC with the One Sample Ahead Preview (OSAP) control law, a particular case of a one step forward MPC controller, for the current loop of a voltage source converter connected to the grid..

2. GRID-CONNECTED CONVERTER WITH LCL

Conversion and electrical energy control by using power converters are important topics of research today. This is due the fact of the increasing energy demands and new requirements in terms of power quality and efficiency.

The renewable energy system is described by the natural source of power, converter, AC filter and capacitor bank. In Fig. 1, the complete system is presented. Here, it's represented renewable energy power system as a continuous-voltage source. Furthermore, it's approximate the grid to a sinusoidal source v_d in series with an inductance L_{g2} and parasitic resistance R_{g2}, assuming that it is predominantly inductive. In addition, LCL filter is represented by the Thevenin equivalent in relation to the PCC (Point of Common Coupling) Tambara et al. (2017). Their parameters, shown on Fig. 1, are i_c, v_c and i_g are converter-side currents, capacitor voltage and grid-side currents, respectively. In addition, C, L_g and R_g are the capacitance of the LCL filter and total grid-side inductance and total grid resistance, respectively.

The grid-connected converter by LCL filter model is highly coupled if it's considered a representation in *abc* coordinates. Design a control method for coupled systems is a complex task. Moreover, if the plant has uncertainties and is subjected to parametric variations, it turns harder the control design. Then, here, the Clarke Transform Duesterhoeft et al. (1951) was applied on *abc* coordinates three-phase coupled model, obtaining two identical decoupled single-phase models in $\alpha\beta 0$ coordinates, Tambara et al. (2017). The equivalent circuits of single-phase models are shown on Fig. 2. These models are linear time-invariant (LIT) and assuming that grid phases are balanced, then the 0 axis can be disregarded, once there will be no path for current flow.

$$\boldsymbol{T}\alpha\beta = \frac{2}{3}\begin{bmatrix} 1 & -1/2 & -1/2 \\ 0 & \sqrt{3}/2 & -\sqrt{3}/2 \\ 1/2 & 1/2 & 1/2 \end{bmatrix} \tag{1}$$

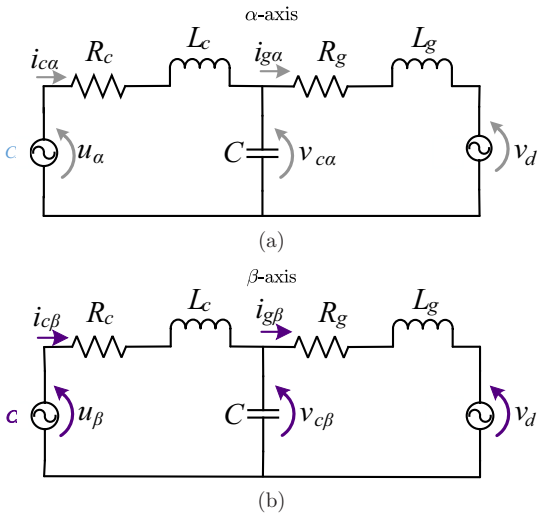

Figure 2. Equivalent circuit of grid-connected voltage-fed three-phase converter with LCL filter: (a) α axis, (b) β axis filter

The identical decoupled single-phase models, $G(s)$, considering $v_d = 0$, are shown on (2).

$$G(s) = \frac{i_g(s)}{u(s)} = \frac{\frac{1}{L_g L_c C}}{s^3 + \frac{(R_g L_c + R_c L_g)}{L_g L_c} s^2 + \frac{(L_c + L_g + R_g R_c C)}{L_g L_c C} s + \frac{R_g + R_c}{L_g L_c C}} \tag{2}$$

where $u(s)$ the voltage synthesised by converter. To do it, a Space Vector Modulation (SVM) was implemented. Moreover, digital implementation delay was considered in the simulation and modelled as an 1 step time delay on control action.

3. CONTROL STRUCTURE AND ADAPTATION ALGORITHM

Considering a linear, time-invariant SISO plant:

$$G(z) = G_0(z)\left[1 + \mu\Delta_m(z)\right] + \mu\Delta_a(z) \tag{3}$$

and $G_0(z)$ as

$$G_0(z) = k_p\frac{Z_0(z)}{R_0(z)} \tag{4}$$

and a model reference in the form

$$W_m(z) = \frac{b_m}{s + a_m} = \frac{y_m(z)}{r(z)} \tag{5}$$

from (1), it's defines a reduced model of the LCL Filter as

$$G_0(z) = \frac{b}{z - a} = \frac{y(z)}{u(z)} \tag{6}$$

whose values of b e a describe the dynamic of plant's real pole.

Rewriting (6) being

$$zy(z) - ay(z) = bu(z) \tag{7}$$

Which implementable form results in

$$y(k+1) = ay(k) + bu(k) \tag{8}$$

or

$$y(k) = ay(k-1) + bu(k-1) \tag{9}$$

From (8), it's desired to obtain a relation whose control law is able to match the plant output with the reference model output: $y(k+1) = y_m(k+1)$; so

$$u(k) = \frac{y(k+1) - ay(k)}{b} \tag{10}$$

Introducing (9) in (11), and replacing $y(k+1)$ by $y_m(k+1)$

$$u(k) = \frac{y_m(k+1) - a(ay(k-1) + bu(k-1))}{b} \tag{11}$$

As shown in (7), rewrites (5) as being:

$$y_m(k+1) = a_m y_m(k) + b_m r(k) \tag{12}$$

Rewriting (12) in (11) and organizing the terms, it obtain,

$$\frac{b}{b_m}u(k) - \frac{ab}{b_m}u(k-1) - \frac{a^2}{b_m}y(k-1) + \frac{a_m}{b_m}y_m(k) + r(k) = 0 \tag{13}$$

No loss of generality, consider $b_m = 1$, and replacing the coefficients that multiply the internal signals of the system by adaptive gains $\boldsymbol{\theta}^T$, it achieves the following control law:

$$\theta_1 u(k) + \theta_2 u(k-1) + \theta_3 y(k-1) + \theta_4 y_m(k) + r(k) = 0 \tag{14}$$

thence,

$$\boldsymbol{\theta}^T(k)\boldsymbol{\omega}(k) + r(k) = 0 \tag{15}$$

For rejection of exogenous disturbance, it is necessary to include in the control law, phase voltage signals $V_s(k)$ and quadrature $V_c(k)$, this components are described by

$$V_s(k) = A_s sin(\omega_{ds} k T_s + \phi_s) \tag{16}$$

and

$$V_c(k) = A_c cos(\omega_{dc} k T_s + \phi_c) \tag{17}$$

Where A, ω_d and ϕ are amplitude, frequency and phase of $V_s(k)$ and $V_c(k)$ component, respectively.

Therefore, the equation (14), turns

$$\begin{aligned}\theta_1 u(k) + \theta_2 u(k-1) + \theta_3 y(k-1)...\\ ... + \theta_4 y_m(k) + \theta_s V_s(k) + \theta_c V_c(k) + r(k) = 0\end{aligned} \tag{18}$$

with

$$\boldsymbol{\theta}^T = [\,\theta_1(k)\ \theta_2(k)\ \theta_3(k)\ \theta_4(k)\ \theta_s(k)\ \theta_c(k)\,]$$

and

$$\boldsymbol{\omega}^T = [\,u(k)\ u(k-1)\ y(k-1)\ y_m(k)\ V_s(k)\ V_c(k)\,]$$

The parametric adaptation law used to tune online the gains of this proposed controller is the Gradient algorithm, similar to Ioannou and Tsakalis (1986b)

$$\boldsymbol{\theta}(k+1) = (\mathbf{I} - \sigma\boldsymbol{\Gamma}T_s)\boldsymbol{\theta}(k) - T_s\kappa\frac{\boldsymbol{\Gamma}\boldsymbol{\zeta}(k)\epsilon_1(k)}{\bar{m}^2(k)} \tag{19}$$

where $\boldsymbol{\Gamma}$ is a positive symmetric matrix gain given as $\gamma\mathbf{I}$, κ is a positive scalar gain, the tracking error $e_1 = y - y_m$, augmented error $\epsilon_1 = e_1 + \boldsymbol{\theta}^T\boldsymbol{\zeta} - W_m(\boldsymbol{\theta}^T\boldsymbol{\omega})$, $\boldsymbol{\zeta} = W_m\mathbf{I}\boldsymbol{\omega}$ is a regression vector whose signals of vector $\boldsymbol{\omega}(k)$ is filtered by reference model and

$$\bar{m}^2(k) = m^2(k) + \boldsymbol{\zeta}^T(k)\boldsymbol{\Gamma}\boldsymbol{\zeta}(k) \tag{20}$$

where the majorant signal $m(k)$ it's calculated as

$$m(k+1) = (1 - T_s\delta_0)m(k) + T_s\delta_1(|u(k)| + |y(k)|) \tag{21}$$

where $m(0) \geq \delta 1/(1 - \delta 0)$.

Moreover, the σ-modification, Ioannou and Tsakalis (1986a) is also used in the adaptation law, is given as follows,

$$\sigma(k) = \begin{cases} 0 & if \ ||\boldsymbol{\theta}(k)|| < M_0 \\ \sigma_0(\frac{||\boldsymbol{\theta}(k)||}{M_0} - 1) & if \ M_0 \leq ||\boldsymbol{\theta}(k)|| \leq 2M_0 \\ \sigma_0 & if \ ||\boldsymbol{\theta}(k)|| > 2M_0 \end{cases} \quad (22)$$

where σ_0 is the maximum value of $\sigma(k)$, M_0 is an upper bound of $||\theta^*||$ and $M_0 > 2||\boldsymbol{\theta}^*||$.

As usual, the value of $||\boldsymbol{\theta}(k)||$ is unknown, M_0 is chosen large enough.

The control and adaptive structure block diagram proposed is shown on Fig. 3

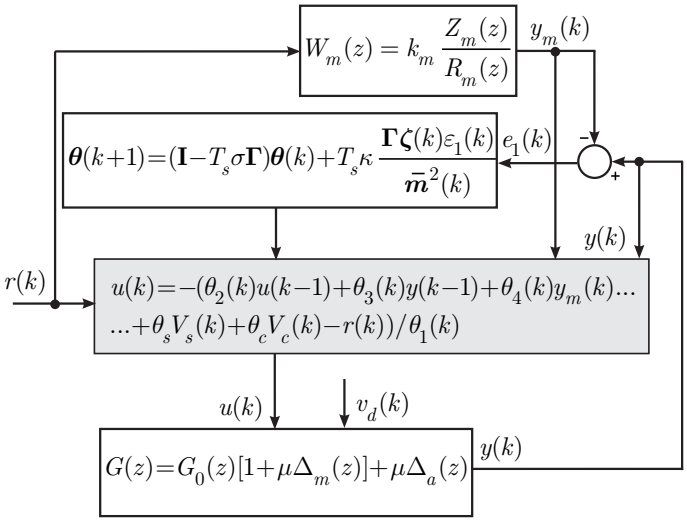

Figure 3. Block diagram of control and adaptive structure

4. CONTROLLER DESIGN

In this section, a design example is given for a 5,2-kW three-phase grid-connected converter with LCL filter, whose parameters are presented in Table 1. The design project considers, as shown in the development of the control law section, a reduced model for the plant, which makes the stability and convergence of the system, a major challenge for the control law.

To implement the presented adaptive algorithm in a digital system, the following 9 steps are executed in a sampling period T_s:

1)Sampling of the PCC three-phase voltages v_{ab} and v_{bc}, two line AC currents in the converter side (i_{ca} and i_{cb}), two line AC voltages in the capacitor C (V_{an} and V_{bn}), two line AC currents in the grid (i_{ga} and i_{gb}) and the voltage in DC link (V_{cc});
Then in $\alpha\beta$ coordinates:
2) Updating of the reference $r(k)$;
3) Updating of the reference model output: $y_m(k)$;
4) Updating of $\boldsymbol{\zeta}(k)$;
5) Updating of $\sigma(k)$
6) Uptading of augmented error $\epsilon(k)$;
7) Uptading of the signal $\bar{m}^2(k)$;
8) Uptading of control action $u(k)$;
9) Uptading of control gains vector: $\boldsymbol{\theta}(k+1)$;

Thus, in each sampling time the action control $u(k)$ is calculated for the modulation of the converter, in *abc* coordinates.

Table 1. System parameters

	Symbol	Parameters	Value
Base Values	V_{cc}	DC link	$400V$
	v_d	Grid voltage	$127V$
	f	Switching frequency	$5kHz$
LCL Filter	L_c	Converter-side inductance	$1mH$
	R_c	Converter-side resistance	$50m\Omega$
	C	Capacitance of LCL Filter	$62\mu f$
	L_{g1}	Grid-side inductance	$0.3mH$
	R_{g1}	Grid-side resistance	$50m\Omega$

By using the parameters presented in Table 1, the resulting transfer function is given by:

$$G(s) = \frac{i_g(s)}{u(s)} = \frac{5,376 \times 10^{10}}{s^3 + 216,7s^2 + 6,99 \times 10^7 s + 5,376 \times 10^9} \quad (23)$$

The Eq. 26 demands a complex adaptive system to be implemented. In order to simplify the development and design of the control structure it's considered simplified first order plant whit dynamics at the frequencies of interest (low frequencies), as described in the controller structure Eq. 6, where the LCL resonance peak is disregarded in the simplified plant. The equation representing the simplified plant is expressed as

$$G_0(s) = \frac{7,69257 \times 10^2}{s + 76,9257} \quad (24)$$

The Fig. 4 show the bode diagram of the simplified plant and real plant

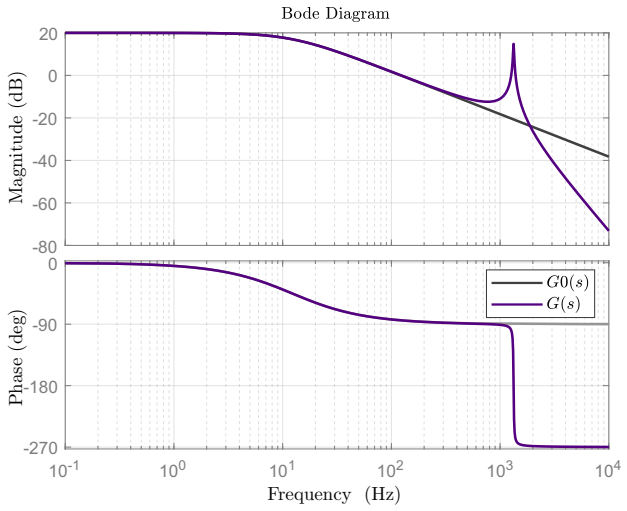

Figure 4. Bode plot of $G_0(s)$ (simplified dynamic plant) and G(s)(completed dynamic plant)

Thus, considering the simplified plant, the model reference, can also be first order which is chosen as:

$$Wm(s) = \frac{1507}{s + 1507} \quad (25)$$

That is discretized with a sampling time of $T_s = 1/5000$

$$Wm(z) = \frac{0.2602}{z - 0.7398} \quad (26)$$

The reference $r(k)$ of grid-current injected chosen for this project was a sinusoidal signal with $10A$, $60Hz$, $0°$ of Amplitude, Frequency and Phase respectively.

Furthermore, in order to evaluate control performance, a $1mH$ inductance with $50m\Omega$ of parasitic resistance, in series with the grid is triggered at a certain instant, causing a parametric variation over the grid impedance,

The bode diagram, Figure 5 shows the open loop frequency response of the reference model, and the plant transfer function considering a parametric variation of grid-side inductance L_{g2} from $0.3mH$ to $1mH$. Note that the position of the resonant peak changes because the position of the poles and zeros depend on the grid impedance. However, the close-loop poles are defined to be located at the same place even with parametric uncertainty or variation. Hence, the gains are adaptly changed to ensure this behavior.

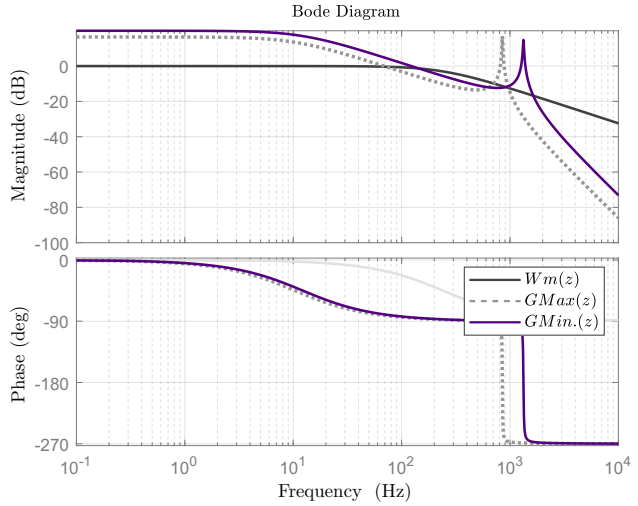

Figure 5. Bode plot of $W_m(z)$(desired closed-loop system) and of $G(z)$ (open loop plant) for different grid inductance

In practice, before starting the close-loop operation, some control parameters must be initialized. As it is possible to have some idea about the grid impedance at the PCC, the initial gains $\boldsymbol{\theta}(0)$ can be found from the matching condition Poh Chiang Loh and Holmes (2005) by assuming, for instance, the parameter Lg_2 with the nominal value as in Table 1.

The Table 2 presents the initial values and definitions of design controller

Table 2. Design controller parameters

Symbol	Value
$\boldsymbol{\theta}(0)$	[-1 0 0 0 0 0]
Γ	10
κ	60
$\sigma 0$	0.1
$M0$	15
$\bar{m}^2$	4
$\delta 0$	0.7
$\delta 1$	1
$\boldsymbol{\zeta}(0)$	[0 0 0 0 0 0]

5. SIMULATIONS RESULTS

In this section, some simulation results are given to demonstrate the performance of the proposed controller that was implemented in PSIM software for grid current control of the three-phase with LCL Filter, as shown in Figure 1.

The dynamic system and controller parameters are presented in Table 1 and 2 respectively, however, to avoid a large transient response, controller gains, $\boldsymbol{\theta}(0)$, in $\alpha\beta$, were initiated and chosen as the final values of a previous simulation, to avoid excessive overshoot in the initial transitory regime, while gains are adapting. It is highlighted that the only gain that must be initialized with correct signal is $\theta_1(0)$, to avoid division by zero.

The Figure 6 shows the adaptation of the gains, to values shown below, in the α and β axis, during the initialization of the system:

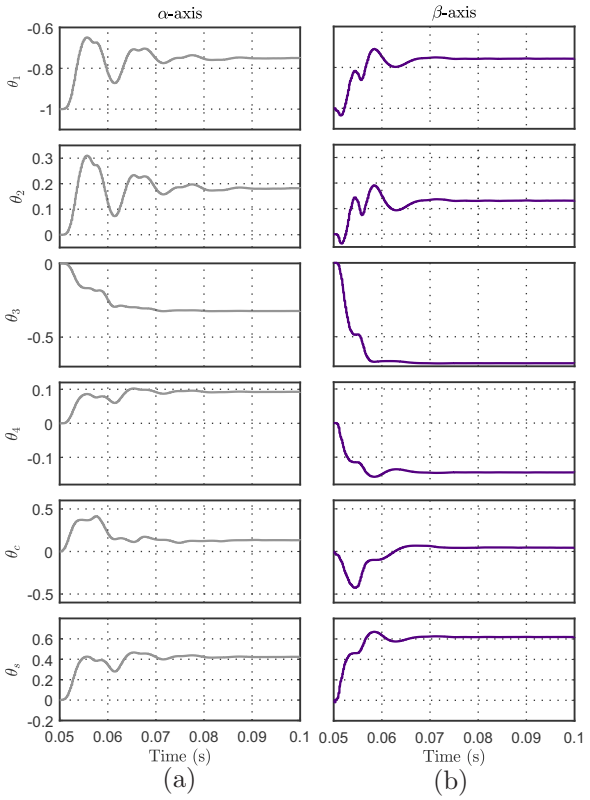

Figure 6. Adaptation of the gains during initialization. (a) α-axis, (b) β-axis

These gains are:

$$\boldsymbol{\theta\alpha}(0) = \begin{bmatrix} -0.73565596 \\ 0.25063896 \\ -0.38088176 \\ 0.042796385 \\ 0.086722091 \\ 0.42407233 \end{bmatrix}, \quad \boldsymbol{\theta\beta}(0) = \begin{bmatrix} -0.74094743 \\ 0.23399849 \\ -0.52122390 \\ -0.51915631 \\ 0.063335113 \\ 0.52586472 \end{bmatrix}$$

The Figures 7 and 8 show, in $\alpha\beta$-axis, the output of plant and the reference model (y and y_m), the control action (u), the augmented and tracking error (ϵ_1 and e_1). The controller performance can be checked against initial

transient response, parametric variation and amplitude variation.

At $t = 0$ second, the synchronization of the converter with the grid is initialized. At $t = 0,05$ seconds, the converter starts the operation with active power reference current.

At $t = 0,15$ second, a transient response occurs for a parametric variation in grid-side inductance L_{g2}, from $0,3mH$ to $1mH$. Note that the controller has a good transient response.

At $t = 0,2$ second, a transient response due to an active power step reference current change from $10A$ to $20A$. It can be seen that the tracking and augmented errors have a reasonable transient response, against this abrupt variation in the current reference. The controller is capable to deal with it and the gains have converged to values close to $\boldsymbol{\theta}^*$ making the output of the plant follow the output of the reference model, taking the error to zero in steady state. After $t = 0,3$ second, the amplitude reference current is set to $10A$ again.

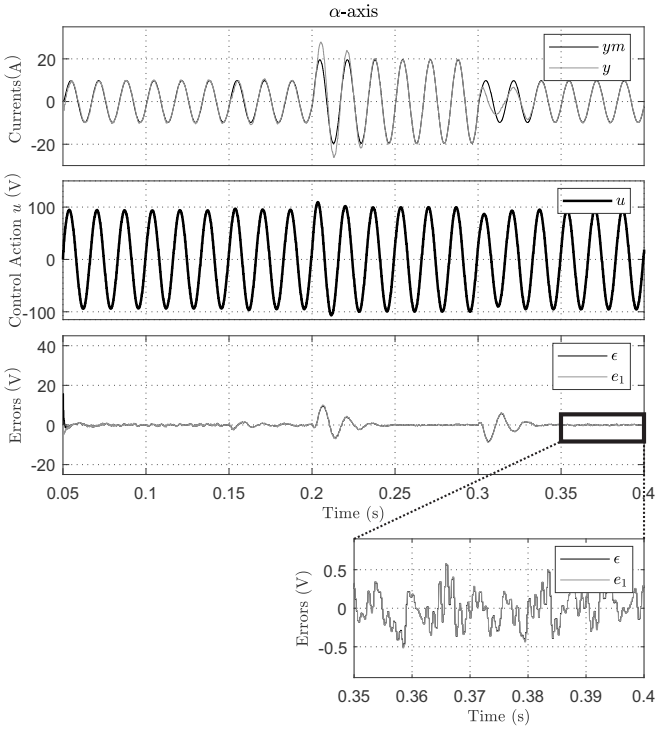

Figure 7. Simulation Results. Transient response of parametric and amplitude variation in α axis

The Figure 9 shows the adaptation of the gains during the startup. It can be reported that there is not a large variation in gains in the initial transient response, due to controller starts with adapted gains. Furthermore, it's possible to notice a similarity in the adaptation of the gains in the α and β axis. As for the characteristics and intrinsic structure of the controller, there is a greater effort to adapt gains to a variation in the amplitude of the reference current compared to parametric variation.

The Figure 10 shows the currents in ABC coordinates for the example simulation proposed, it can check that the adaptive current controller for grid-connected converter application can ensure fast transient response and

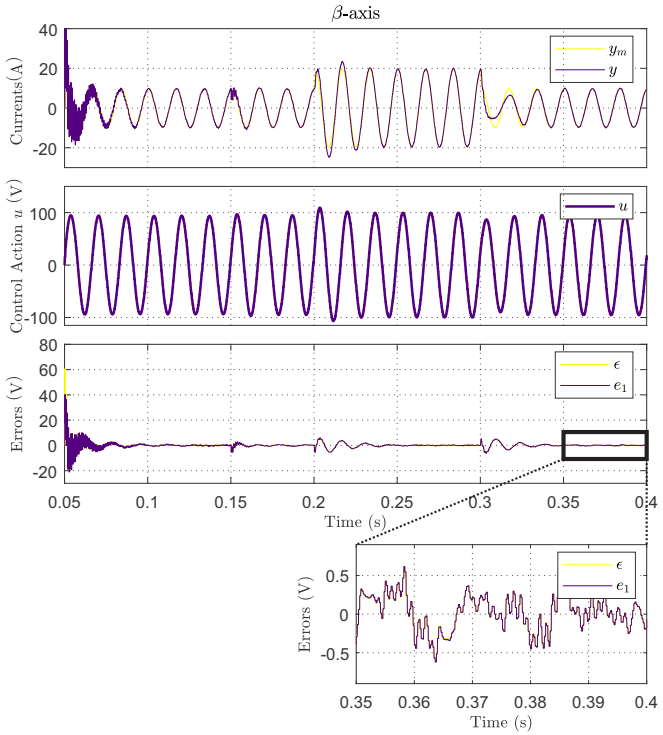

Figure 8. Simulation Results. Transient response of parametric and amplitude variation in β axis

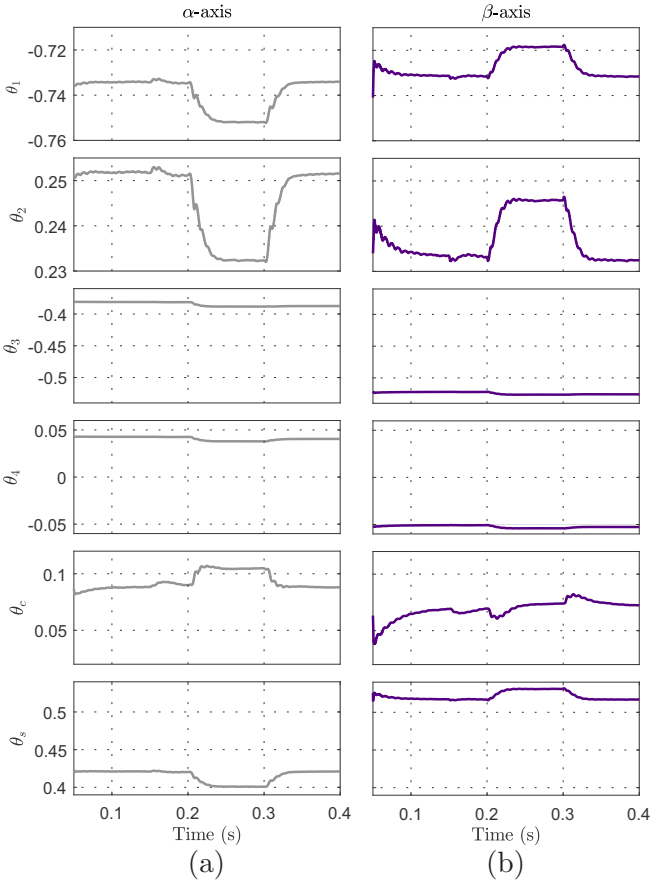

Figure 9. Simulation Results. Adaptation of the feedback gains during the startup. (a) α-axis, (b) β-axis

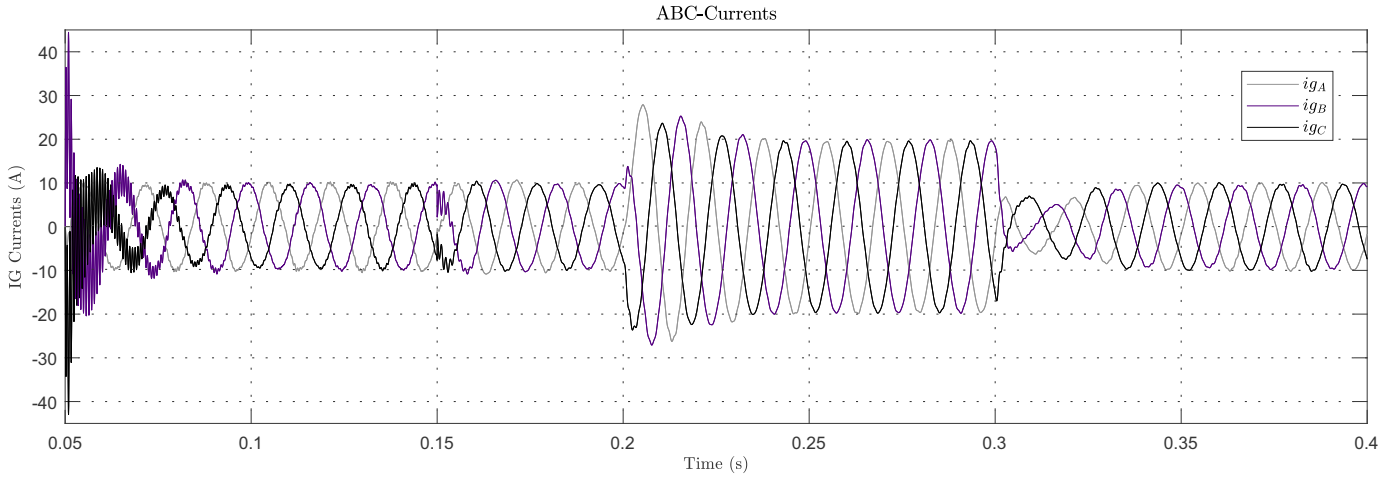

Figure 10. Simulation results. Transient response of parametric and amplitude variation in *ABC* coordinates

good steady-state performance, even without knowledge of the equivalent grid impedance at the PCC. Moreover, the current-controlled grid-connected converter with LCL filter has the fast response imposed by the reference model, which is not dependent on the grid.

6. CONCLUSIONS

This paper presents a discrete-time adaptive current controller for grid-connected voltage source converters with LCL filter. It showed that the proposed adaptive algorithm provides a good performance in reference tracking as well as in disturbance rejection even under parametric variation and abrupt changes in the reference. The simulation results pointed out the effectiveness of the design procedure which it was main feature for the successful implementation of the adaptive controller.

ACKNOWLEDGMENT

To the Brazilian agencies CAPES and CNPq - Finance Code 001. CAPES 88887.479774/2020-00.

REFERENCES

Baek, J., Kim, S., and Kwak, S. (2015). Predictive control method for load current of single-phase voltage source inverters. In *2015 IEEE Applied Power Electronics Conference and Exposition (APEC)*, 2256–2260.

Chen, J.W., Liu, Y.C., et al. (2019). Design of dc microgrid system for integration of pmsm elevator and renewable energy sources. In *2019 IEEE 10th International Symposium on Power Electronics for Distributed Generation Systems (PEDG)*, 981–985. IEEE.

Chowdhury, V.R. (2016). Analysis control and design of a hybrid renewable power generation system. In *North American Power Symposium (NAPS)*, 1–7. IEEE.

Dannehl, J., Fuchs, F.W., and Hansen, S. (2007). Pwm rectifier with lcl-filter using different current control structures. In *2007 European Conference on Power Electronics and Applications*, 1–10. IEEE.

Duesterhoeft, W.C., Schulz, M.W., and Clarke, E. (1951). Determination of instantaneous currents and voltages by means of alpha, beta, and zero components. *Transactions of the American Institute of Electrical Engineers*, 70(2), 1248–1255.

Exposto, B., Rodrigues, R., Pinto, J.G., Monteiro, V., Pedrosa, D., and Afonso, J.L. (2015). Predictive control of a current-source inverter for solar photovoltaic grid interface. In *2015 9th International Conference on Compatibility and Power Electronics (CPE)*, 113–118.

Fang, X., Ding, X., Zhong, S., and Tian, Y. (2019). Improved quasi-y-source dc-dc converter for renewable energy. *CPSS Transactions on Power Electronics and Applications*, 4(2), 163–170.

Gabe, I.J., Montagner, V.F., and Pinheiro, H. (2009). Design and implementation of a robust current controller for vsi connected to the grid through an lcl filter. *IEEE Transactions on Power Electronics*, 24(6), 1444 – 1452.

Ioannou, P.A. and Tsakalis, K.S. (1986a). A robust direct adaptive controller. *IEEE Transactions on Automatic Control*, 31(2), 1033 – 1043.

Ioannou, P.A. and Tsakalis, K.S. (1986b). A robust discrete-time adaptive controller. *IEEE Proceedings of 25th Conference on Decision and Control*, (2), 1033 – 1043.

Jha, S. (2016). Implication of optimal performance of renewable energy system. In *7th Power India International Conference (PIICON)*, 1–5. IEEE.

Kuznietsov, M., Vyshnevska, Y., Brazhnyk, I., and Melnyk, O. (2019). Modeling of the generation-consumption imbalance in the heterogeneous energy systems with renewable energy sources. In *6th International Conference on Energy Smart Systems (ESS)*, 196–200. IEEE.

Lindgren, M. and Svensson, J. (1998). Control of a voltage-source converter connected to the grid through an lcl-filter-application to active filtering. *Proceedings of PESC'98*, 229 – 235.

Liserre, M., Teodorescu, R., and Blaabjerg, F. (2006). Stability of photovoltaic and wind turbine grid-connected inverters for a large set of grid impedance values. *IEEE Transactions on Power Electronics*, 21(1), 263–272.

Maccari, L.A. ; Massing, J..S.L..R.C..P.H..O.R..F.M.V. (2014). Lmi-based control for grid-connected converters with lcl filters under uncertain parameters. *Power Electronics, IEEE Transactions on*, 29, 3776–3785.

Malinowski, M., Milczarek, A., Kot, R., Goryca, Z., and Szuster, J.T. (2015). Optimized energy-conversion systems for small wind turbines: Renewable energy sources in modern distributed power generation systems. *IEEE*

Power Electronics Magazine, 2(3), 16–30.

Mariethoz, S., Beccuti, A.G., and Morari, M. (2008). Analysis and optimal current control of a voltage source inverter connected to the grid through an lcl filter. *Records of IEEE Power Electronics Specialists*, 2132 – 2138.

Massing, J., Stefanello, M., Gründling, H., and Pinheiro, H. (2012). Adaptive current control for grid-connected converters with lcl-filter. *Industrial Electronics, IEEE Transactions on*, 59, 4681 – 4693.

Mohamed, Y.R. and El-Saadany, E. (2007). An improved deadbeat current control scheme with a novel adaptive self-tuning load model for a three-phase pwm voltage-source inverter. *IEEE Trans. Ind. Electron.*, 54(2), 747 – 759.

Poh Chiang Loh and Holmes, D.G. (2005). Analysis of multiloop control strategies for lc/cl/lcl-filtered voltage-source and current-source inverters. *IEEE Transactions on Industry Applications*, 41(2), 644–654.

Ponnaluri, S. and Serpa, L. (2008). Dc/ac converter with dampened lcl filter distoritions. *United States Patent*, (US7450405B2).

Shi, H., Zong, J., and Ren, L. (2019). Modified model predictive control of voltage source inverter. In *2019 IEEE 4th Advanced Information Technology, Electronic and Automation Control Conference (IAEAC)*, volume 1, 754–759.

Tambara, R.V. (2014). *Um controlador adaptativo robusto aplicado a conversores estáticos conectados à rede elétrica através de filtro LCL*. Ph.D. thesis, Universidade Federal de Santa Maria, UFSM.

Tambara, R.V., Massing, J.R., Pinheiro, H., and Gründling, H.A. (2013). A digital rmrac controller based on a modified rls algorithm applied to the control of the output currents of an lcl-filter connected to the grid. *European Power Electronics conference (EPE)*.

Tambara, R.V., Kanieski, J.M., Massing, J.R., Stefanello, M., and Gründling, H.A. (2017). A discrete-time robust adaptive controller applied to grid-connected converters with lcl filter. *Journal of Control, Automation and Electrical Systems*, 28(3), 371–379.